Preprint
UCRL-JC-144458

Effects of Helium on Radiation Damage Processes in Iron

K. Morishita, B. D. Wirth, T. Diaz de la Rubia, A. Kimura

This article was submitted to
4th Pacific Rim International Conference on Advanced Materials and Processing, Honolulu, HI, December 1, 2001

June 2, 2001

This work was performed under the auspices of the United States Department of Energy by the University of California, Lawrence Livermore National Laboratory under contract No. W-7405-Eng-48.

Effects of Helium on Radiation Damage Processes in Iron

Kazunori Morishita[1, *], Brian D. Wirth[2], Tomas Diaz de la Rubia[2], Akihiko Kimura[1]

[1] *Institute of Advanced Energy, Kyoto University, Uji, Kyoto 611-0011, Japan*
[2] *Lawrence Livermore National Laboratory, University of California, Livermore, California 94550, USA*

Molecular dynamics calculations were performed to evaluate the energies of helium-related defects in α-iron for investigation of helium behavior during irradiation. The interatomic potentials employed here were the Ackland Finnis-Sinclair N-body potential, the Wilson-Johnson potential and the ZBL-Beck potential for describing interactions of Fe-Fe, Fe-He and He-He, respectively. The migration energy of interstitial helium is extremely low, indicating that an interstitial helium atom can migrate rapidly in the metal even at extremely low temperature, until the helium atom is trapped or escapes outside. One of the most efficient trapping sites for helium is a vacancy or small vacancy clusters (nanovoid). The formation energy of helium-vacancy clusters in iron was calculated as a function of the number of helium atoms and vacancies. The binding energy of an interstitial helium atom, a substitutional helium atom and a vacancy to the cluster was also determined as a function of the helium-to-vacancy ratio of the cluster. Helium is strongly bound to the helium-vacancy cluster, and it can stabilize the cluster, thereby increasing cluster lifetime by dramatically reducing thermal vacancy emission. The binding of helium and vacancies to a helium-vacancy cluster greatly depends on the helium-to-vacancy ratio of the cluster. For clusters with extremely high helium-to-vacancy ratios, it was observed that the collective motion of helium atoms produces bubble pressures large enough to spontaneously create additional vacancies and associated self-interstitial atoms at the periphery of the cluster. Finally, the possibility of athermal production of self-interstitial atom (SIA) loops (i.e., dislocation loop punching) from the cluster is discussed.

Keywords: *molecular dynamics (MD), molecular statics (MS), iron (Fe), helium (He), helium-vacancy cluster, SIA-loop punching*

1. Introduction

The introduction of helium into metals by direct helium implantation or by nuclear (n, α)-reactions during neutron irradiation can produce significant changes in metal microstructure and properties. In the fusion energy environment, high rates of insoluble helium are generated concurrently with radiation damage. Therefore, understanding helium behavior in metals remains one of the most important subjects in the field of research and development of nuclear fusion reactor materials.

High helium concentrations and the formation of helium bubbles in metals are known to enhance void swelling and produce surface roughening and blistering, and high temperature intergranular embrittlement [1]. The energetics and formation kinetics of helium-vacancy clusters and helium bubbles provides the basis for understanding helium effects in metals. In the present study, we report the results of atomistic simulations, namely molecular dynamics (MD) and molecular statics (MS), performed to calculate the formation energies of helium-vacancy clusters.

2. MD simulation and interatomic potentials

Molecular dynamics (MD) calculations were performed to investigate helium behavior in α-iron. Interatomic potentials employed here were the Ackland potential [2], the Wilson-Johnson potential [3] and the Beck potential [4] to describe interactions of Fe-Fe, Fe-He and He-He, respectively. The Ackland potential is a many-body type interatomic potential described within the Finnis and Sinclair framework [5], while the other two potentials simply include pairwise interactions. The Wilson-Johnson potential is purely repulsive and derived from Hartree-Fock-Slater (HFS) calculations using the modified Wedepohl method [6]. The Beck potential for He-He interactions was smoothly connected with the Ziegler-Biersack-Littmark (ZBL) universal potential [7] that is appropriate at high energy (short interatomic separations). These interatomic potentials indicate that an equilibrium volume per atom and corresponding cohesive energy per atom are 0.0118 nm^3 and –4.316 eV for perfect bcc Fe, and 0.0172 nm^3 and –0.00714 eV for perfect fcc He, respectively.

In the present calculations to evaluate the formation energy of vacancy-helium clusters, MD simulations were performed at ~300K for 10 picoseconds (using the 0K lattice parameter), followed by quenching to 0 K and a final relaxation to zero pressure. The defect formation energy is obtained by comparing the total potential energy of a perfectly ordered crystal containing the appropriate number of atoms and the computational cell containing the defect. Using this procedure, the formation energy and volume of a vacancy in α-iron was calculated to be 1.70 eV and 0.81 Ω_{Fe}, where Ω_{Fe} is the equilibrium volume per atom in perfect bcc iron. These values are consistent with those previously reported by Ackland et al. [2]. In the present calculations, three-dimensional periodic boundary conditions were employed and the computational box was 10 *a* x 10 *a* x 10 *a*, where *a* is the lattice parameter. This box size is large enough to evaluate cluster energies and, in fact, the number of atoms treated here was much larger than that of the calculations of Adams et al. for He-vacancy clusters in nickel [8].

3. Helium atom formation and migration

The diffusion coefficients of interstitial helium in α-iron were calculated from the helium mean squared displacement in MD simulations over a temperature range of 100 to 1100 K using the relation,

$$D_{He} = \left\langle \left\{ r_{He}(t + \Delta t) - r_{He}(t) \right\}^2 \right\rangle \Big/ 6\Delta t, \quad (1)$$

where $\boldsymbol{r}_{He}(t)$ is the position vector of helium at time t. The

---

* *Associate Professor, Institute of Advanced Energy, Kyoto University, Gokasho, Uji, Kyoto 611-0011, Japan, TEL +81 774 38 3477, FAX +81 774 38 3479, morishita@iae.kyoto-u.ac.jp*

Arrhenius plot of the diffusion coefficients provides an activation energy for interstitial helium diffusion of 0.078 eV. Although the equilibrium volume per atom of solid fcc helium is larger than that of bcc iron, helium can migrate very rapidly through the iron lattice, moving three-dimensionally between the various bcc interstitial positions. Molecular statics simulations reveal that the octahedral interstitial position (O-site) is the most stable site for helium in an otherwise perfect α -iron lattice, and that helium migration occurs from an O-site to an equivalent O-site via the tetrahedral interstitial position (T-site). The formation energy of interstitial helium at the octahedral and tetrahedral positions is 5.25 eV and 5.34 eV, respectively. The energy difference between the two positions (0.085 eV) is nearly identical to the interstitial helium migration energy obtained through MD simulations.

The formation energy of a substitutional helium atom is 3.25 eV and thus, the binding energy of helium to a vacancy is 3.70 eV. This large binding energy indicates that helium is deeply trapped by a vacancy and suggests that helium detrapping from a vacancy will not occur, except at significantly high temperatures. The possible diffusion of substitutional helium is expected to occur by a vacancy mechanism, and, under irradiation with high vacancy supersaturations, it is likely that the substitutional helium migration energy will be nearly the same as for an isolated vacancy (0.74 eV). In fact, the energy for moving a substitutional helium atom into a neighboring vacancy is extremely small (about 0.015 eV) and thus, an activation energy of ~0.75 eV can be expected for substitutional helium migration under irradiation.

4. Helium-vacancy cluster formation

Fig. 1 plots the formation energy of a helium-vacancy cluster (He_nV_m) relative to perfect bcc iron and fcc helium crystals, where *n* and *m* are the numbers of helium atoms and vacancies in the cluster, respectively.

We find that the calculated formation energy of a vacancy cluster without helium (n=0), e.g. an 'empty' nanovoid, is well fit by an empirical relationship proposed by Si-Ahmed and Wolfer [9]

$$E_{void}^{f} = 4\pi R^2 \gamma \left\{1 - 0.8/(m+2)\right\}, \qquad (2)$$

where R is the void radius and γ is the average formation energy of a flat surface. Although eq. (2) is constructed from rather macroscopic considerations, it agrees very well with the formation energy of nanovoids as small as one vacancy, as was also observed by Adams and Wolfer for the case of nickel [8]. We obtain a value of 10.54 eV/nm^2 for the surface energy, γ, by fitting to the calculated formation energy of a nanovoid containing 20 vacancies. This value of γ agrees well with the energy calculated for low index (110), (100) and (111) surfaces using the Ackland interatomic potential, with values of 9.86, 11.45 and 12.46 eV/nm^2, respectively.

Increasing the helium content in small helium-vacancy clusters drastically increases the formation energy of the cluster. For a given number of helium atoms, the lowest energy configuration has one vacancy per helium atom. This behavior is the same as observed by Adams and Wolfer for helium-vacancy clusters in fcc nickel [8]. When the helium-to-vacancy ratio of a cluster is less than about 1 (n/m < 1), the formation energy of the cluster is close to the void formation energy described by eq. (2). However, when n/m > 1, the energy increase due to the presence of helium is very large. In this way, the cluster size dependence of the formation energy of a helium-vacancy cluster is greatly dependent on the fraction, n/m.

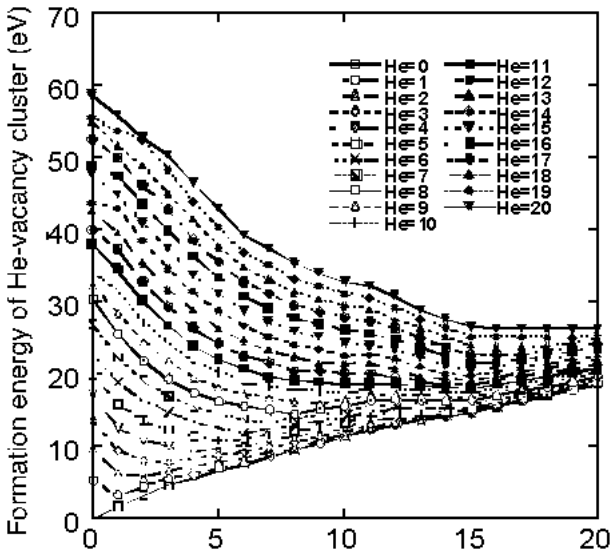

Fig. 1 Formation energy of a helium-vacancy cluster (He_nV_m) relative to a perfect bcc iron crystal with a perfect fcc helium crystal.

It is interesting to note that the formation energy of a divacancy in bcc Fe is higher for first-nearest neighbor vacancy pair (3.26 eV) than that of the second-neighbor pair of vacancies (3.22 eV), as is usually found in stable bcc metals. However, for a divacancy-helium complex, the lowest energy configuration of the vacancy pair depends on the number of helium in the divacancy. For up to eight helium atoms, the formation energy of a divacancy-helium complex for the first-nearest neighbor vacancy pair is lower than that for the second-nearest neighbor pair, while, for more than nine helium atoms, the energy difference between them becomes more complicated and it strongly depends on the number of helium atoms in the complex, as shown in Table 1. Interestingly, for a first nearest-neighbor vacancy pair-helium complex, the He atoms are located in the interstitial positions between the two vacant sites, while for a second nearest-neighbor vacancy pair, the He atoms cluster close to each lattice site. In Fig. 1, the lowest energy configuration of the He-vacancy pair is depicted.

The formation energies of small helium-vacancy clusters are quite low (that is the binding energies are quite high), even at relatively large helium-to-vacancy ratios. It is interesting that both the binding energies and atomic volumes of helium atoms in helium-vacancy clusters in iron are significantly larger and smaller, respectively than the cohesive energy (~ 7 meV) and atomic volume (1.46 Ω_{Fe}) of

a close-packed helium lattice. The binding energies and volume dependence can easily be explained by the difference in interactions between the two atoms; the repulsive interaction between Fe-He is simply much greater than the relatively weak He-He interaction of a closed shell noble gas. Thus, the energetically favorable helium clustering in iron and other metals occurs through a decrease in the number of high energy, repulsive Fe-He interactions (bonds). Specifically for the divacancy-helium complexes discussed above, the number of Fe-He interactions for the complex of second-nearest neighbor vacancies is larger than that of the first-nearest neighbor vacancies because of the helium distribution described above.

5. Possibility of SIA loop punching

We have investigated the potential for the spontaneous creation of self-interstitial atoms (SIAs) and prismatic SIA loop punching by high pressure helium bubbles, as first proposed by Trinkaus and Wolfer [10]. For small clusters with extremely high helium to vacancy ratios (i.e., a higher helium density cluster), the collective motion of helium atoms has been observed to spontaneously create additional vacancies and corresponding SIAs that remain at the cluster periphery. For example, when an additional helium atom is bound to a pre-existing He_6V cluster, the helium can push a lattice atom off its normal site, resulting in creation of an SIA-vacancy pair. Such an SIA-vacancy pair, however, energetically prefers to remain in the near vicinity of the cluster. This observation is consistent with the earlier work of Wilson et al. [11]. In general, the cluster cannot emit an isolated SIA because the formation energy price to create an isolated SIA is too high (4.88 eV). Likewise, an even higher formation energy exists for creating an isolated helium interstitial (5.25 eV). In our results, even as the helium to vacancy ratio approached 20, the production of an isolated SIA was not observed and indeed is not energetically favorable and requires thermal activation.

However, the production of a prismatic SIA loop is different. Consider the following reaction of SIA loop production,

$$He_n \rightarrow He_nV_m + I_m, \qquad (3)$$

where I_m denotes an *m*-size SIA loop, and compare the formation energies of defects between the left- and right-hand sides. Fig. 2 shows the sum of formation energy of a He_nV_m cluster and that of an *m*-size SIA loop, I_m. At m=0, Fig. 2 represents the formation energy of a He_n cluster. For helium-vacancy clusters with a low helium density, the sum of the formation energies is a monotonically increasing function of the value, *m*, and it is, therefore, always higher than the He_n formation energy, indicating that SIA loop production is an energetically unfavorable process. However, for clusters with higher helium density ($N \geq 11$), eq. (3) can become energetically favorable. For example, the energetics of Fig. 2 show that a He_{20} cluster can decrease the total energy by producing a 5-17 SIA loop. It should be emphasized here that investigation of the minimum-energy geometry of these clusters shows that the SIAs always prefer to cluster on the same side of the helium-vacancy cluster, consistent with Wilson's observation [11], which indicates that clustering of pushed-off lattice atoms takes place at the periphery of the helium-vacancy cluster. However, the energetics of Figure 2 clearly show that for high helium to vacancy ratios and certain size SIA loops, the loop can be energetically punched out to form an isolated loop. Such an athermal SIA loop production results in production of the same number of vacancies at the helium-vacancy cluster, and thus effectively decreases the helium-to-vacancy ratio of the cluster. In this way, the cluster may become an embryonic helium bubble.

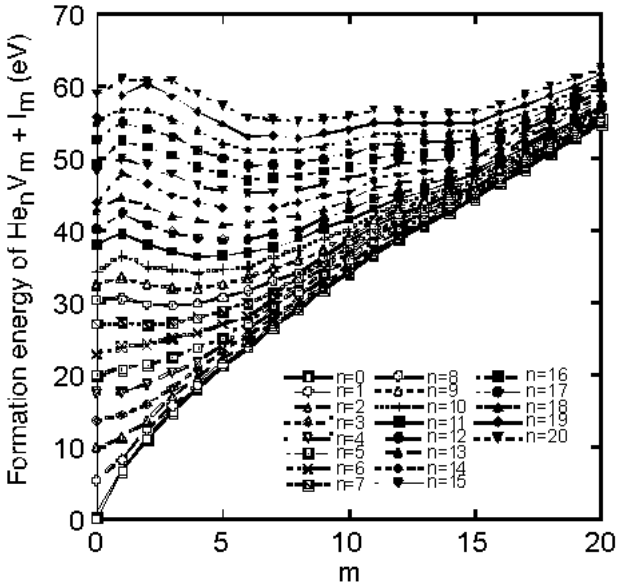

Fig. 2 Sum of formation energies of a He_nV_m cluster and an *m*-size SIA loop, I_m as a function of *m*. For greater n/m values, it suggests athermal production of loop.

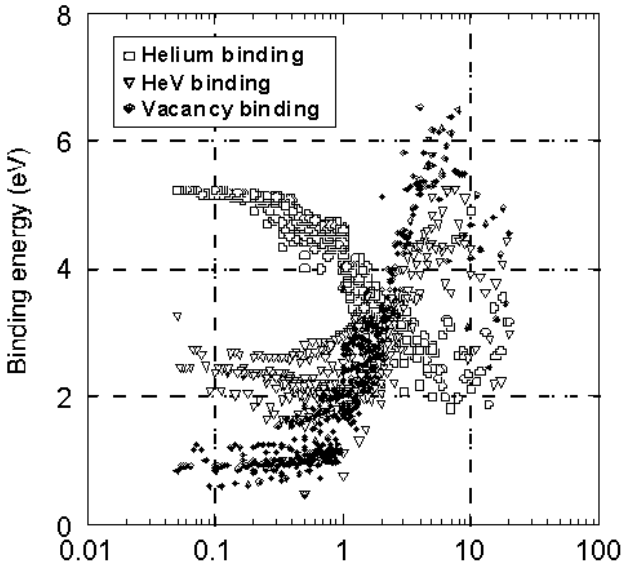

Fig. 3 Various binding energies as a function of helium-to-vacancy ratios.

Table 1 The formation energy of a divacancy-helium complex as a function of the number of helium atoms in the complex. The divacancy has two types of vacancy configuration in bcc lattice: first and second nearest-neighbor vacancy pairs, which are indicated by 1nn and 2nn, respectively.

#He	0	1	2	3	4	5	6	7	8	9	10
1nn	3.26	4.49	5.77	8.09	10.87	13.59	16.32	19.04	21.95	24.73	27.17
2nn	3.22	4.77	6.22	8.66	11.44	14.17	16.89	19.40	21.99	24.65	27.25
#He	11	12	13	14	15	16	17	18	19	20	
1nn	30.27	33.46	35.49	40.32	41.10	44.14	46.96	49.57	52.46	52.95	
2nn	30.20	33.00	36.49	38.65	41.14	43.74	46.29	48.95	52.91	53.98	

6. Binding energy

Fig. 3 plots the binding energies of helium atoms (He, $E_{He}^{b(I)}(m,n)$), helium-vacancy complexes (HeV, $E_{He}^{b(S)}(m,n)$) and vacancies (V, $E_V^b(m,n)$) to a helium-vacancy cluster (He_nV_m) as a function of the helium-to-vacancy ratio of the cluster. Following Adams and Wolfer [8], the binding energies were defined by the following equations,

$$E_{He}^{b(I)}(m,n) = E_{He}^{I} + E^f(m,n-1) - E^f(m,n), \quad (4)$$

$$E_{He}^{b(S)}(m,n) = E_{He}^{S} + E^f(m-1,n-1) - E^f(m,n), \quad (5)$$

$$E_V^b(m,n) = E_V^f + E^f(m-1,n) - E^f(m,n), \quad (6)$$

where E_{He}^{I}, E_{He}^{S}, E_v^f and $E^f(m, n)$ are the formation energy of interstitial helium, substitutional helium, a vacancy and a helium-vacancy cluster of *m* vacancies with *n* helium atoms, respectively. The binding energies of HeV and V to the cluster show basically increasing functions of helium-to-vacancy ratio (i.e., helium density), while the He binding energy shows basically a decreasing function.

Thermal helium desorption experiments during annealing after 8 keV helium ion bombardment in pure iron show that the desorption peaks that appear at around 750 K shift to lower temperatures with increasing ion dose [12]. The present calculation may suggest that this experimental desorption peak corresponds to dissociation of interstitial helium atoms from a helium-vacancy cluster, because the helium binding is considered to be a decreasing function of ion dose.

Except for the extremely higher helium density regime, the HeV and V binding energies increase with helium density. This is because removal of a vacancy from a helium-vacancy cluster greatly increases the helium density in the remaining cluster, which increases the energy of the cluster. This effect of helium in smaller helium-vacancy clusters can stabilize the clusters and prevent their decay by thermal vacancy emission.

For the significantly higher helium density above about 5 He/vacancy, the dependence of the binding energies on the helium density changes. In this density regime, the HeV and V binding energies are a decreasing function and the He binding energy is an increasing function of helium density. These behaviors may correspond to athermal production of SIAs and acquiring of corresponding additional vacancies, as discussed above and which results in a decrease in the actual helium density of the cluster.

7. Conclusion

A combined molecular dynamics and molecular statics simulation study was performed to investigate the energetics of helium-vacancy clusters. Isolated, interstitial helium has a very high formation energy (5.25 eV) and very low activation energy for migration (<0.1 eV), but is very strongly trapped by individual vacancies. The energetics of small (He & V ≤ 20) helium-vacancy clusters depends on the ratio of helium to vacancies. For clusters with extremely high helium density (He/V > 10), the athermal production of SIA loops is shown to be energetically favorable.

Acknowledgement

One of the authors (KM) wishes to acknowledge the generous hospitality of Lawrence Livermore National Laboratory during an exchange visit. This work was performed under the auspices of the program from the 'JUPITER' Monbusho-US DOE collaboration and from the US Department of Energy under Contract No. W-7405-Eng-48. The work was also supported by a Grant-in-Aid from the Ministry of Education, Science, Sports and Culture of Japan.

REFERENCES

[1] *See, for example,* E.E. Bloom: J. Nucl. Mater. **258-263** (1998), pp. 7-17; N. Yoshida and Y. Hirooka: J. Nucl. Mater. **258-263** (1998), pp. 173-182.

[2] G.J. Ackland, D.J. Bacon, A.F. Calder, and T. Harry: Philos. Mag., A75 (1997), pp. 713-732.

[3] W.D. Wilson and R.D. Johnson: 'Rare Gases in Metals', in Interatomic potentials and simulation of lattice defects, (Ed. by P.C. Gehlen, J.R. Beeler, Jr., and R.I. Jaffee): Plenum, (1972), pp. 375-390.

[4] D.E. Beck: Mol. Phys. **14** (1968), pp. 311-315.

[5] M.W. Finnis and J.E. Sinclair: Philos. Mag., **A50** (1984), pp. 45-55; **A53** (1986), p. 161 (erratum).

[6] P.T. Wedepohl: Proc. Phys. Soc., 92 (1967) 79.

[7] J.P. Biersack and J.F. Ziegler: Nucl. Instrum. Meth., **194** (1982), pp. 93-100.

[8] J.B. Adams and W.G. Wolfer: J. Nucl. Mater., **166** (1989), pp. 235-242.

[9] A. Si-Ahmed and W.G. Wolfer: Proc. 11th Conf on Effects of Radiation on Materials, ASTM STP **782**, Eds. H.R. Brager and J.S. Perrin (American Society for Testing and Materials, 1982), pp. 1008-1022.

[10] H. Trinkaus and W.G. Wolfer: J. Nucl. Mater., **122&123** (1984), pp. 552-557.

[11] W.D. Wilson, C.L. Bisson and M.I. Baskes: Phy. Rev., **B24** (1981), pp. 5616-5624.

[12] K. Morishita, R. Sugano, H. Iwakiri, N. Yoshida and A. Kimura: The fourth Pacific Rim International Conference on Advanced Materials and Processing (PRICM4), this volume.